J. Fluid Mech. (1990), *vol.* 220, *pp.* 369–395
Printed in Great Britain

Two-phase multicomponent filtration: instabilities, autowaves and retrograde phenomena

By V. S. MITLIN

Institute of Earth Physics of the Academy of Sciences of the USSR, Bol. Gruzinskaya ul. 10,
123810 Moscow, USSR

(Received 30 October 1989)

The different modifications of the models of two-phase multicomponent filtration (Collins 1961; Nikolaevsky *et al.* 1968) enable one to study the dynamics of filtration flows, taking into account phase transitions. The equations of multicomponent filtration are quite complicated and only in a few individual cases do they allow for an exact solution. The most frequently used of these appears to be the solution of the stationary problem of the flow of a multicomponent mixture toward a well or a system of wells (Khristianovich 1941). In the present paper we show that at certain values of pressure, temperature and composition of the multicomponent mixture a stationary solution of the problem may not exist. The absence of a stationary solution is related to the possibility of a spatially homogeneous solution losing its stability under a perturbation (Mitlin 1986*a*, 1987*b*). We obtain an analytical criterion for instability. As an illustration, we present the results of the numerical solution of the planar linear problem of the evolution of a multicomponent system whose pressure and composition are perturbed with respect to their constant values, which are equal at both ends. We have done a numerical analysis of the plane-radial problem of the operation of a gas–condensate well with different mass fluxes, applying the conditions of a real deposit. There are several ranges of flux where the flow becomes pulsating. It is shown that the time within which the stationary solution sets in is a non-monotonic function of flux and on approaching the stability limit diverges in inverse proportion to the undercriticality of debit. We have analysed the connection between the observed instabilities and the thermodynamics of two-phase multicomponent mixtures. It is shown that the instabilities are associated with the system entering the region of retrograde condensation. We discuss the relation of retrograde phenomena to the effect of negative volume of heavy components and, as a consequence, to the negative compressibility of an individual volume of a two-phase mixture moving in a porous medium. It is shown that the observed autowave modes are relaxation oscillations in a distributed system. By using the method of perturbations in the interphase equilibrium time, we have analysed the loss of stability in a more general – non-equilibrium – model. We show that the instabilities are generated according to the Landau–Hopf scenario and calculate the period of auto-oscillations. The one-mode approximation of the theory leads to the Van der Pol equation. In conclusion we present an experimental confirmation of the theory.

1. Introduction

In the present paper we consider one of the possible scenarios according to which the stationary regimes of two-phase multicomponent filtration may lose their stability and, as a consequence, according to which autowaves may appear. Pulsatory filtration regimes are constantly encountered by engineers when they study the exploitation of oil–gas–condensate deposits. The observed pulsations may be caused by the action of non-monotonic or periodic external forces (Moon, earthquakes, microseismic action, etc.). Such effects will not be considered here. We shall be interested in a situation where there is a time-monotonic (e.g. constant) inflow of energy into an open system, which, owing to its own nonlinearity, transforms the incoming energy into oscillations. We shall also be interested in the conditions (bifurcational values of the parameters) under which branching of the solution occurs and the stationary regime is replaced by the autowave. Such effects are studied by synergetics (Haken 1983). This approach is rather general: the specific aim of our present study is to find the relation between the observed instabilities and typical features of phase diagrams for multicomponent mixtures. In our scenario the autowaves are associated with the cyclic changing of the following processes: the increase of the volume occupied by the liquid phase (condensation); the flow of the liquid as it becomes sufficiently mobile in the porous medium; and the diminishing of the volume occupied by the liquid phase (evaporation). Correspondingly, the instability of conditions are equivalent to the conditions of the system being in the region of retrograde condensation. We shall discuss in detail the relation between retrograde phenomena and the so-called effect of negative volume of heavy components. It will be shown that there is a direct connection between these phenomena and the negative compressibility of an individual volume of the filtrating two-component continuum and that this is what leads to instability. It is shown that, mathematically, the loss of stability occurs via Hopf bifurcation and that the autowaves are relaxation oscillations in a distributed system. Finally, we discuss the results of recent experiments to check the predictions of the considered theory. These experiments have confirmed the correctness of our theoretical concepts (Mitlin 1986*a*, 1987*b*).

2. Initial equations and stability conditions

Assuming that the process is isothermic; that the generalized Darcy law for phases is valid; that the gravitation, diffusion and capillary forces are small; and that there is local thermodynamical equilibrium between phases, let us consider a system of filtration equations for a two-phase l-component mixture (Collins 1961; Nikolaevsky *et al.* 1968):

$$m\frac{\partial N z_i}{\partial t} = \nabla\cdot(k\beta_i\nabla P), \quad i = 1, \dots, l, \tag{2.1}$$

$$\beta_i = \frac{f_\mathrm{g}\rho_\mathrm{g}}{\mu_\mathrm{g} M_\mathrm{g}} y_i + \frac{f_\mathrm{w}\rho_\mathrm{w}}{\mu_\mathrm{w} M_\mathrm{w}} x_i, \quad N = S\frac{\rho_\mathrm{w}}{M_\mathrm{w}} + (1-S)\frac{\rho_\mathrm{g}}{M_\mathrm{g}}.$$

In (2.1) $P(\boldsymbol{r},t)$ is pressure, $z_i(\boldsymbol{r},t)$ is the mole fraction of the ith component in the mixture,

$$\sum_{i=1}^{l} z_i = \sum_{i=1}^{l} y_i = \sum_{i=1}^{l} x_i = 1, \tag{2.2}$$

$k(\boldsymbol{r})$ and $m(\boldsymbol{r})$ are the absolute permeability and porosity; $f_\mathrm{g}, f_\mathrm{w}$, $\rho_\mathrm{g}, \rho_\mathrm{w}$, and $\mu_\mathrm{g}, \mu_\mathrm{w}$ are respectively the permeabilities, densities and viscosities of the phases; y_i and x_i are mole fractions of the ith component in the gaseous and the liquid phases;

$M_g = \sum_{i=1}^{l} M_i y_i$ and $M_w = \sum_{i=1}^{l} M_i x_i$ are the average molecular weights of the gaseous and the liquid phases; M_i is the molecular weight of the ith component,

$$\frac{y_i}{x_i} = K_i \tag{2.3}$$

where K_i is the equilibrium constant of the ith component; S is the saturation of the porous medium by the liquid phase; V is the mole fraction of the gaseous phase,

$$\sum_{i=1}^{l} \frac{(K_i - 1) z_i}{1 + V(K_i - 1)} = 0, \quad S = \frac{(1-V)\rho_g M_w}{(1-V)\rho_g M_w + V\rho_w M_g}, \tag{2.4}$$

r is the radius vector of a space point, and t is time.

In the above formulation, (2.1)–(2.4), of the problem the unknown quantities are P and z_i $(i = 1, \ldots, l-1)$. All the rest of the quantities are expressed through pressure and total composition. Indices g and w label respectively the gaseous and the liquid phases. This formulation of the problem and this choice of basic variables are most convenient for the mathematical simulation of multicomponent filtration (Aziz & Settari 1979).

Let k and m be constant. Let us consider the linear stage of evolution of the perturbation of a spatially homogeneous solution in the region that has the form of a rectangular parallelepiped. As it is usually done when one studies hydrodynamical fluctuations, let us impose periodic boundary conditions at the boundary of this region. Owing to the autonomy of system (2.1)–(2.4), this corresponds to spatially periodic initial conditions for the problem considered here. In the case of an arbitrary region, after one isolates the time derivatives of P and z_i in the initial equations, one should expand the solution in eigenfunctions of the differential operator on the right-hand sides of the linearized equations, which, in this case, are complex exponents.

Let us present (2.1) as

$$\nabla \cdot (k\beta_i \nabla P) = m\left(N\frac{\partial z_i}{\partial t} + z_i \frac{\partial N}{\partial t}\right), \quad i = 1, \ldots, l. \tag{2.5}$$

By summing (2.1) we get

$$\nabla \cdot (k\beta \nabla P) = m\frac{\partial N}{\partial t}, \quad \beta = \sum_{i=1}^{l} \beta_i. \tag{2.6}$$

Substituting (2.6) into (2.5) and performing simple transformations, in the linear approximation we obtain

$$\frac{\partial P'}{\partial t} = I\nabla^2 P', \quad \frac{\partial z_i'}{\partial t} = (\beta_i - z_i\beta)\frac{k}{mN}\nabla^2 P', \quad i = 1, \ldots, l-1, \tag{2.7}$$

where $P' = P(r,t) - P^0$, $z_i' = z_i(r,t) - z_i^0$, and index '0' denotes the spatially homogeneous solution.† In what follows, the quantity

$$I = \frac{k}{m}\left(\frac{\partial N}{\partial P}\right)^{-1}\left[\beta - \sum_{j=1}^{l-1} \frac{1}{N}\frac{\partial N}{\partial z_j}(\beta_j - z_j\beta)\right] \tag{2.8}$$

will be called the increment of stability of a spatially homogeneous solution.

---

† From (2.7) it follows that P' and z_i' are related as $z_i' = k(\beta_i - z_i\beta)P'/mNI$.

The growth (or dying-out) of Fourier components of P' and z_i' is determined by the eigenvalues of the linear response matrix of the system (2.1):

$$\left.\begin{aligned} &\boldsymbol{A} = \{a_{ij}\}: \quad a_{il} = -\frac{k}{mN}q^2(\beta_i - z_i\beta), \quad 1 \leqslant i \leqslant l-1; \\ &a_{ll} = -q^2 I; \quad a_{ij} = 0, \quad j < l. \end{aligned}\right\} \tag{2.9}$$

From (2.9) it follows that matrix $\boldsymbol{A}$ has $l-1$ identically zero eigenvalues and one non-zero eigenvalue $\lambda_l = -q^2 I$. Here $q^2 = 4\pi^2 \sum_{j=1}^{d} L_j^{-2}$ is the wave vector squared, L_j is the size of the region in the jth direction, and d is the dimension of the region. By virtue of Lyapunov's theorem (Marsden & McCraken 1976), the sufficient condition of instability of a spatially homogeneous solution is

$$I < 0. \tag{2.10}$$

The possibility of losing stability essentially has to do with the multicomponent system having more than one phase. Indeed, in the one-phase case (for example, at $V = I$) we have $\beta_i = z_i\beta, i = 1, \dots, l-1$, and (2.10) is equivalent to the condition $\partial\rho_g/\partial P < 0$, which corresponds to thermodynamical instability of the one-phase system and contradicts the initial assumption of the theory. Let us now show that when there are several liquids flowing without mixing with one another, condition (2.10) cannot be satisfied either. For simplicity, let us consider the system of equations for two-phase filtration. For a larger number of liquids the calculations become more cumbersome but are performed in exactly the same way. We have

$$m\frac{\partial}{\partial t}(\rho_w S) = \boldsymbol{\nabla}\cdot\left(\frac{k\rho_w f_w}{\mu_w}\boldsymbol{\nabla} P\right), \quad m\frac{\partial}{\partial t}(\rho_g(1-S)) = \boldsymbol{\nabla}\cdot\left(\frac{k\rho_g f_g}{\mu_g}\boldsymbol{\nabla} P\right). \tag{2.11}$$

By linearizing system (2.11) with respect to the spatially homogeneous solution and solving it with respect to P' and S', one finds that the stability of a non-perturbed solution is determined by the eigenvalues of the matrix $\boldsymbol{A} = \{a_{ij}\}$:

$$a_{11} = a_{21} = 0, \quad a_{22} = -\frac{k}{m}\frac{q^2\rho_w\rho_g(f_w/\mu_w + f_g/\mu_g)}{\rho_g S\,\partial\rho_w/\partial P + \rho_w(1-S)\,\partial\rho_g/\partial P}.$$

One of these eigenvalues is identically zero; the other is a_{22}. One can easily see, however, that a_{22} is always negative.

Let us finally note that when deriving condition (2.10) we made use of the dependence of N on P. When searching for analytical solutions of equations of multicomponent filtration one often makes the assumption that the mixture is incompressible or that the sum of partial volumes of components is constant – the Amague law (Barenblatt, Entov & Ryzhik 1984), which results in $\partial N/\partial P = 0$. In our case, if N is independent of P, the linearization gives $\nabla^2 P' = 0$, the system of linearized equations becomes degenerate and the linear approximation becomes non-informative.

Condition (2.10) can also be used for determining the regions of instability of stationary solutions in the case where one introduces into (2.1) terms that correspond to sources and sinks of sufficiently small power. This is a consequence of the fact that the positive eigenvalue λ_l changes little with a small variation of boundary conditions and of the equations themselves. Thus, the filtration modes for which the stationary solution of (2.1) is unstable can be obtained when one 'turns on'

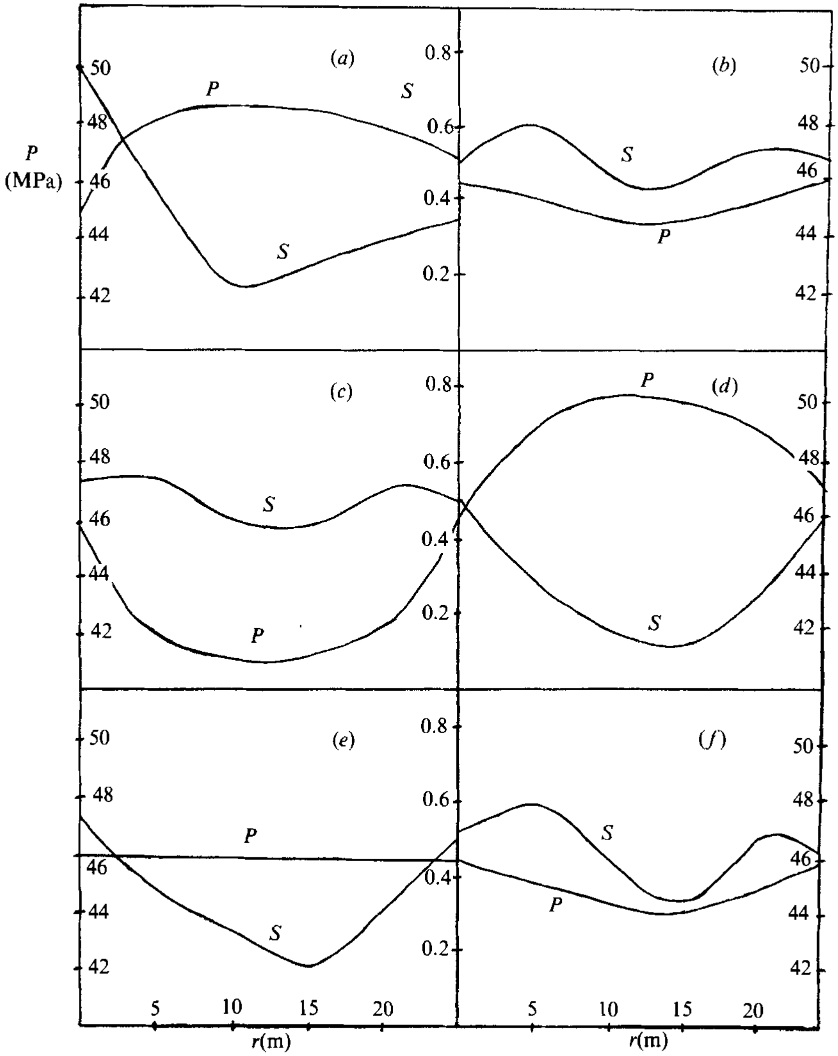

FIGURE 1. Evolution of the perturbation of the space homogeneous state: profiles of P and S. (a) $t = 0$, (b) $t = 2$ days, (c) $t = 4$ days, (d) $t = 10$ days, (e) $t = 14$ days, (f) $t = 30$ days.

sufficiently weak sinks against the background of initial conditions P^0 and z_i^0 such that $I(P^0, z_1^0, \ldots, z_{l-1}^0 < 0$. For condition (2.10) to hold, it is necessary that the multicomponent system has two phases, that its components mix, and that N depends on P.

In order to describe the instabilities that we have observed in the calculations, let us present the results of a numerical solution of the planar linear problem of multicomponent filtration with the condition that the layer pressure at both end points is kept constant and equal to 46 MPa. The initial distribution of P and z_i was perturbed with respect to the spatially homogeneous solution. In the process of calculation, the concentrations at the boundary were not fixed if the flow came toward it; if the flow went away from it, the composition on the boundary was taken from the previous time layer. In the calculations we have taken $k = 10^{-15}$ m^2, $m = 0.1$, $T = 353$ K; the initial composition was: $CH_4 - 0.6926$, $C_2H_5 - 0.0616$, $C_3H_8 - 0.0334$, $iC_4H_{10} - 0.0055$, $nC_4H_{10} - 0.0079$, $N_2 - 0.009$, $H_2S - 0.0625$, $CO_2 - 0.0346$, C_{5+}

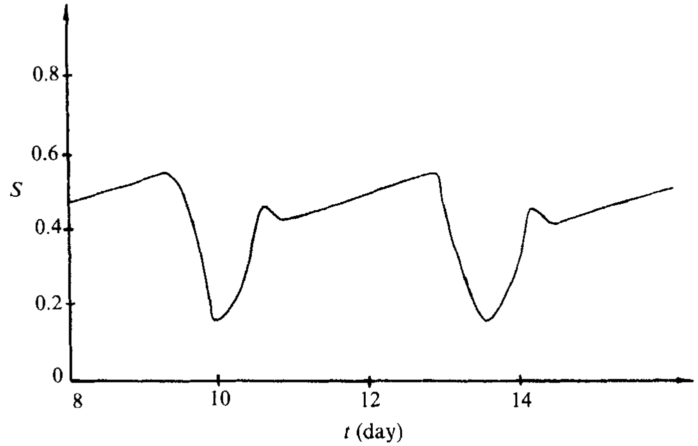

FIGURE 2. The same problem as in figure 1: the dynamics of S is shown in the middle of the solution region.

(pentane and heavier) – 0.0928. These data and a set of fluxes in the next section correspond to conditions of the gas–condensate deposit at Karachaganak (USSR) in 1985.

The equilibrium constants were approximated by some functions of pressure; the density and viscosity of phases were approximated by functions of pressure and of the molecular weights of the phases. The data necessary for constructing these dependences were obtained from preliminary calculations of phase equilibria for the initial mixture and different pressures according to the Peng–Robinson equation of state (Read, Prausnitz & Sherwood 1977). The phase permeabilities were taken to be of the form

$$f_w = \begin{cases} 0, & S \leqslant 0.2, \\ \left(\dfrac{S-0.2}{0.8}\right)^3, & S > 0.2, \end{cases} \qquad f_g = \begin{cases} 0, & S \geqslant 0.8 \\ \left(\dfrac{0.8-S}{0.8}\right)^3, & S < 0.8. \end{cases}$$

Our method of numerical calculation is a more complicated version of the IMPES method for equations of two-phase filtration (Aziz & Settari 1979) for the multicomponent case. The difference scheme is implicit with respect to pressure and explicit with respect to concentrations. In order to reduce the number of calculations we designed a method without the iteration procedures by using the three-layer approximation of time derivatives in (2.1). A more detailed description of the method can be found in Mitlin (1986*b*, 1987*a*).

Figure 1 shows the profiles of P and S at different times. One can see that the solution is pulsating: the convexity of the profile changes. The pulsations of saturation are more interesting: at different times its profile has a different number of extrema. This means that the process involves waves of different wavelength. By comparing figures 1(*b*) and 1(*f*) we see that in the system, a successive change of spatial distributions of S occurs modulated and non-modulated in amplitude. This effect is typical of nonlinear oscillations: for example the Fermi–Pasta–Ulam return phenomenon in the theory of solitons (Yuen & Lake 1978), and the same phenomenon in equations with completely different structure – in the brusselator model with distributed parameters (Nicolis & Prigogine 1977). Figure 2 shows a fragment of the time variation of S in the middle of the solution region.

Calculations show that at each time, the stability increment has a negative value at one or several sites of the difference grid. At the same time, the perturbations with respect to the pressures 43 MPa and 48 MPa and the same composition died out: the system relaxed toward a spatially homogeneous state and at all points of the solution region the stability increment was positive. Thus, we have observed a 'window' in the range of P-variation such that inside that window autowaves are generated in the system. Direct calculations of I for the same composition when P varies show that $I < 0$ exactly in the region $43.5 < P < 47.5$ (see below figure 11). Thus, the test demonstrates that the appearance of autowaves is explained by hydrodynamical (but not numerical) instability.

3. Pulsatory flow regimes of a multicomponent mixture

Below we present the results of the solution of the plane-radial problem of the operation of a gas–condensate well with constant pressure at the boundary of the sink zone. The solution is found in the region $(r_b, R_k), P(r,0) = P(R_k, t) = 55$ MPa and $z_i(r,0) = z_i(R_k, t)$; the initial composition is as presented in the previous section and is kept constant at the boundary of the drain zone. At the well, a constant total mass flux is fixed: $Q = 2\pi hk\beta M_f^{-1} r(\partial P/\partial r)|_{r=r_b}$, where $M_f = \sum_{i=1}^{l} M_i \epsilon_i$ and $\epsilon_i = \beta_i/\beta$ is the mole fraction of the ith component in the flow. The values of k and m and the form of the functions K_i, ρ_g, ρ_w, μ_g, μ_w, f_g, and f_w are the same as in the previous section. The seam thickness is $h = 50$ m, $r_b = 0.12$ m, and $R_k = 25.12$ m.

The results of calculation are presented in table 1 and in figures 3–5. At $Q =$ 50 ton/day and $Q = 70$ ton/day (figure 3*a*) the problem has a stationary solution (the solution was considered stabilized if the pressure and saturation at the well were constant up to the fourth digit within 25 steps in time, i.e. 5 days). At $Q = 86.4$ ton/day the stationary solution lost its stability: after 160 days the smooth variation of parameters was replaced by pulsations. The pressure at the well at that time was 47.1 MPa. At $Q = 100$ ton/day the smooth lowering of pressure at the well was replaced by pulsations after 60 days. The amplitude of pulsations grew up to a certain magnitude, after which the solution transformed into a time-periodic one. The form of the stabilized pressure and saturation pulsations at the well, together with the fraction of gas in the product flow from the well, V_g, and the fraction of heavy components (C_{5+}) in the extracted gas, α_h, are shown in figure 4(*a*). The position of the time zero in figure 4 is not important since the figure shows the behaviour of the solution at large t. The profiles of S corresponding to its extreme values at the well at stabilized oscillations are shown in figure 3(*b*). In the cases where there are no stationary regimes, the stabilization time column, t_s, of the table is left empty, while in the P, S, V_g and α_h columns in these cases we present the values averaged over a period of stabilized oscillations for $r = r_b$. ΔP and ΔS are the doubled amplitudes of stabilized oscillations of pressure and saturation.

At $Q = 160$, 190, and 200 ton/day the stationary solution has existed (figure 3*c*), but the approach to it was accompanied by pulsations which appeared when the pressure at the well reached 47.1 MPa. The pulsations of P at the well appeared between 44 and 38 MPa and gradually disappeared, after which P smoothly fell until the system reached a stationary regime. In these three calculations the pulsation time was maximum at minimum Q, the closest to the interval $86.4 < Q < 100$, within which the pulsations did not die out at all.

At $Q = 210$ ton/day, after the pressure at the well reached 34.9 MPa, a pulsatory regime appeared. At $Q = 240$ ton/day the stationary solution also existed. The form

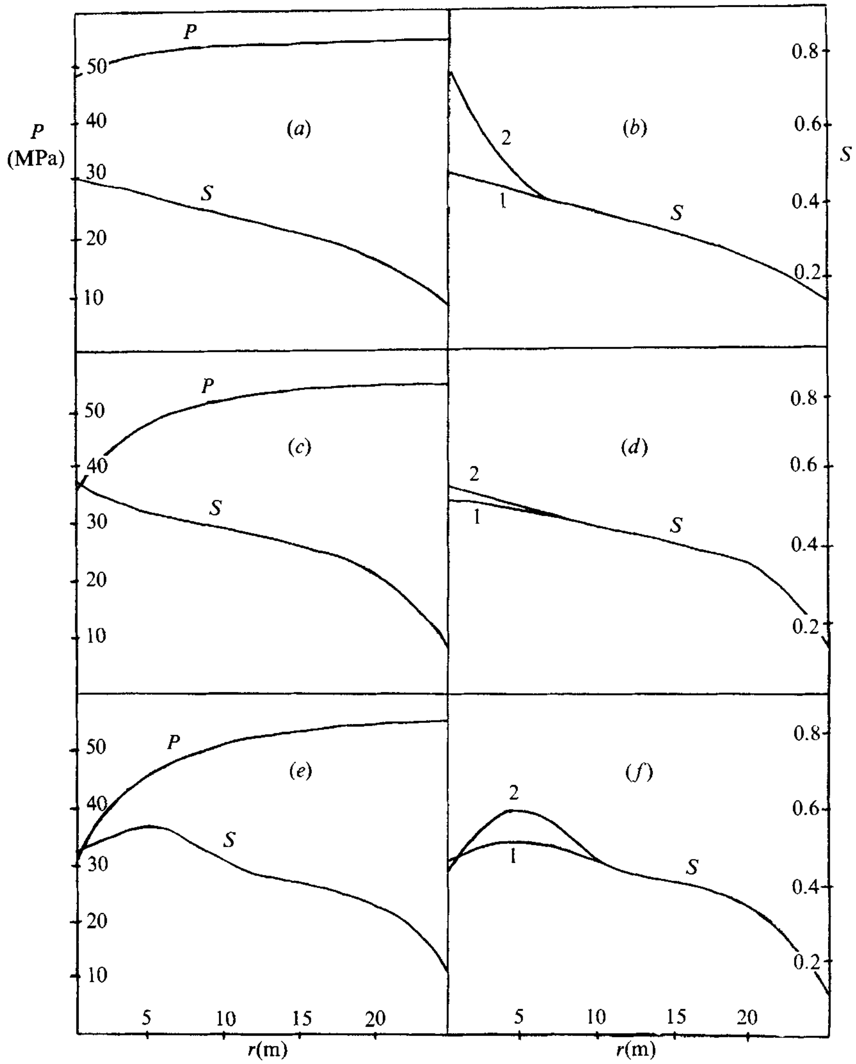

FIGURE 3. Inflow of gas-condensate mixture to a well (for conditions of deposit Karachaganak, USSR). (*a*, *c*, *e*) Stationary solution; steady-state profiles of P and S are shown. (*b*, *d*, *f*) Stationary solution does not exist; profiles of S corresponding to its extreme values at the well at stabilized oscillations are shown. (*a*) $Q = 70$ ton/day, (*b*) $Q = 100$ ton/day, (*c*) $Q = 200$ ton/day, (*d*) $Q = 240$ ton/day, (*e*) $Q = 420$ ton/day, (*f*) $Q = 500$ ton/day.

Q (ton/day)	50	70	100	160	190	200	240	324	420	500	700
t_s (day)	200	400	—	320	320	420	—	160	140	—	—
P (MPa)	52	48.5	46	38.5	36.1	35	33.2	31.3	30.3	30.1	27.8
α_n (%)	7,9	7,1	5,3	4,2	3,4	3,1	2,7	2,2	1,9	2,0	2,1
S (%)	37,5	46,2	62	55,1	55,5	56,3	53,9	50,5	47,5	44	34,1
V_g (%)	98,1	90.5	45,8	75,8	77,8	77	85,3	92,8	96,1	97,8	98,6
ΔP (MPa)	—	—	2,9	—	—	—	1,6	—	—	3,8	17
ΔS (%)	—	—	26	—	—	—	1,7	—	—	2,6	18,9

TABLE 1. The inflow of gas–condensate mixture to a well: results of calculations

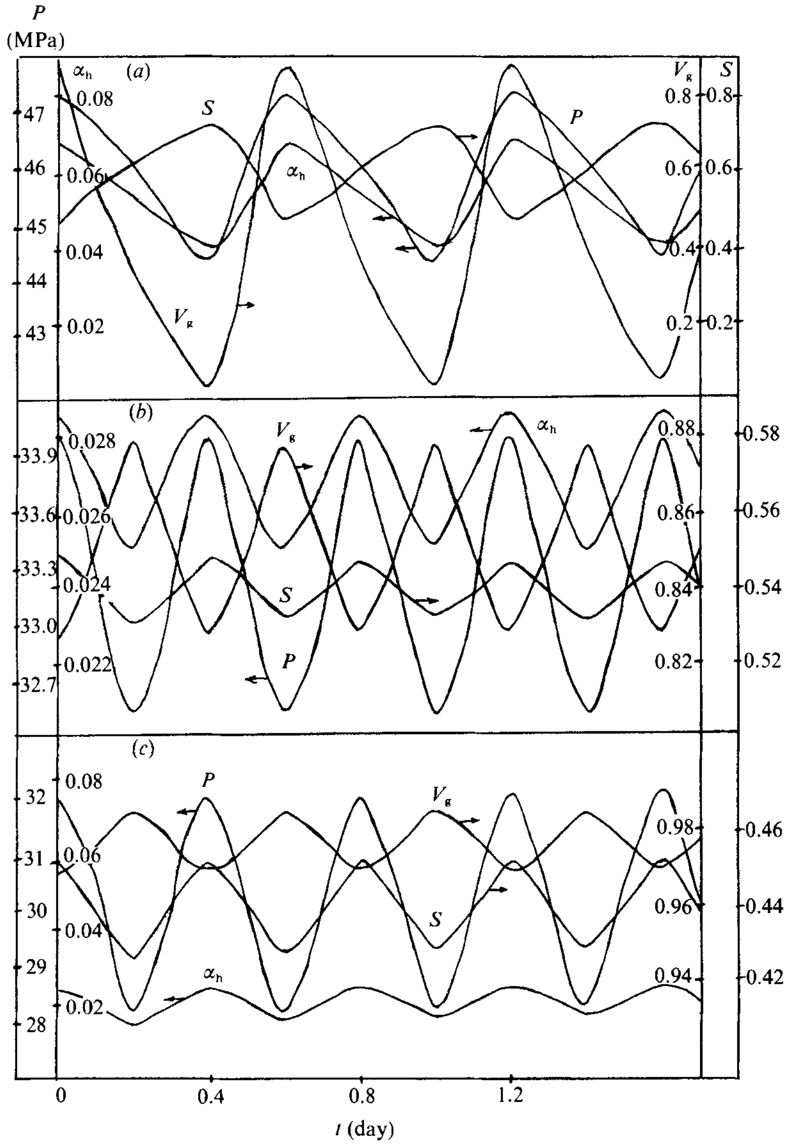

FIGURE 4. The same problem as in figure 3. Oscillations of parameters at the well at large times are shown. (*a*) $Q = 100$ ton/day, (*b*) $Q = 200$ ton/day, (*c*) $Q = 500$ ton/day.

of stabilized pulsations at the well is shown in figure 4(*b*). The profiles of saturation at its extreme values at the well are featured in figure 3(*d*).

At $Q = 324$ and 420 ton/day the stationary solution appeared once again (figure 3*e*). In this case, at the initial stage pulsations appeared, the amplitude of which reached significant values: up to 20 MPa in pressure. The time dependence of P and S at the well during the first 9 days is featured in figure 5. Compared to the pulsations in figure 5(*a*), those in figure 5(*b*) have a noticeable modulation depth. In both of these cases, when the pressure at the well reached 47.1 MPa (the upper limit of the first zone of instability), the saturation sharply changed – the system was 'thrown out' into the stable zone. For some time after that the process went on smoothly and the pressure at the well fell, and then a new change occurred in

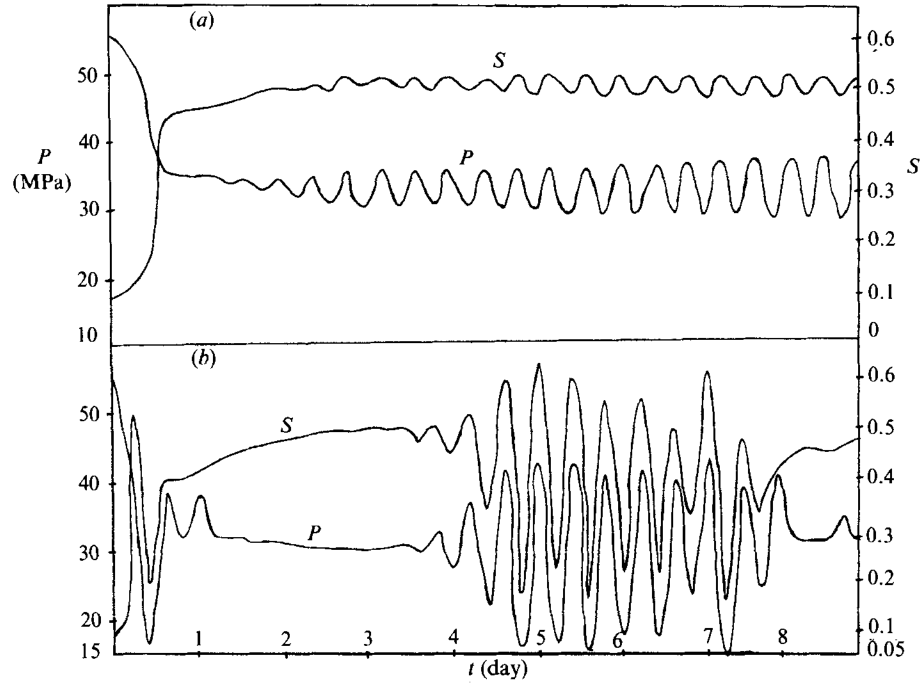

FIGURE 5. Dynamics of P and S at the well during the first 9 days. (a) $Q = 324$ ton/day, (b) $Q = 420$ ton/day.

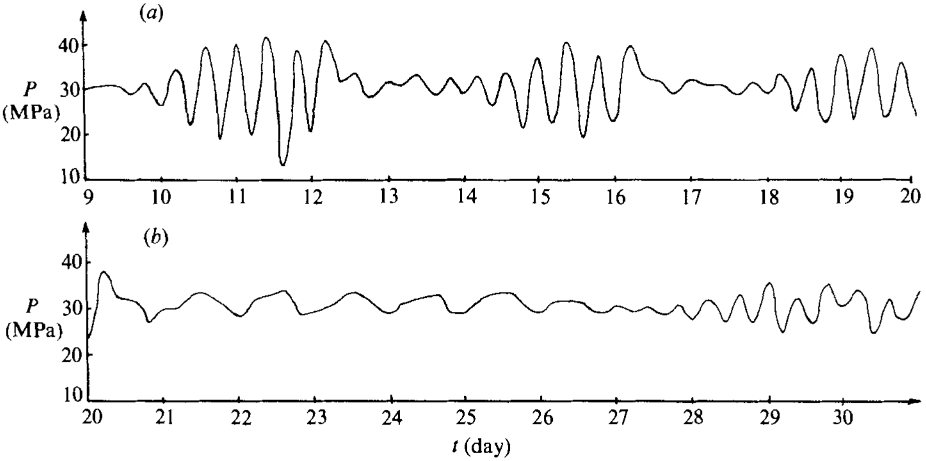

FIGURE 6. The same problem as in figure 5, but when $t > 9$. (a) $Q = 324$ ton/day, (b) $Q = 420$ ton/day.

the pulsatory regime (for $Q = 324$ ton/day this happened at 35 MPa; for $Q = 420$ ton/day at 32 MPa) but in the end the oscillations disappeared. It is interesting to note that at $Q = 420$ ton/day the system approaches the stationary mode in a very complicated manner. Figure 6 shows the variation of pressure at the well at $t > 9$ days. One can see that in the calculations, the flashes of stochastic behaviour (sharp peaks and gaps) alternated with dynamics that was almost periodic

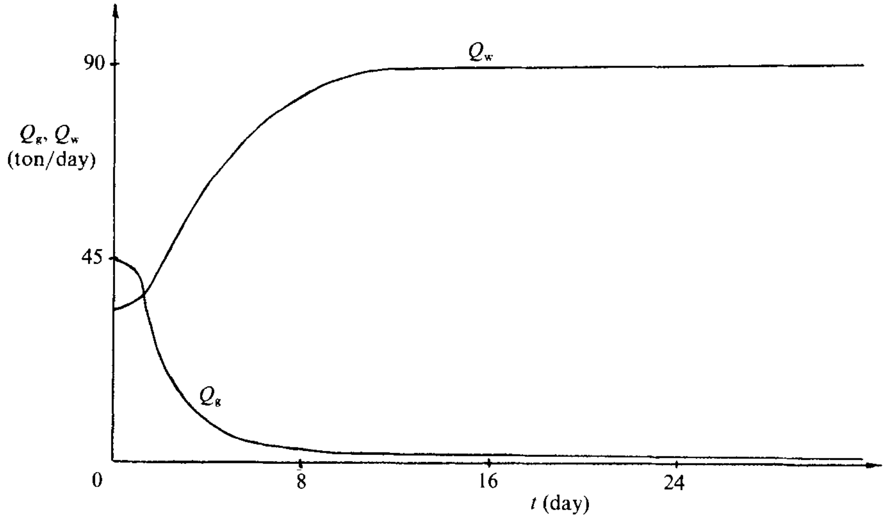

FIGURE 7. Dynamics of phase flux in the problem with pressures of 45 and 55 MPa at the boundaries. Stationary regime exists.

in time. As is well known, such effects have been observed in the scenario of turbulence generation via alternation (Landau & Lifshitz 1986).

At $Q = 500$ and 700 ton/day, at large t one observed stabilized pulsations. As one can see in figure 3(*f*), they involved a larger portion of space than in the case of smaller fluxes. Moreover, periodically, in the vicinity of the well a billow of S forms, which subsequently flattens out.

It should be noted that pulsation generation does not depend on the geometry of the problem: this is shown by the calculations made in the previous section and, also, by the calculations for a planar linear problem with pressure fixed at one end and mass flux at the other. In this case, too, one has observed pulsatory regimes, and the values of parameters of the system at which the stationary solution became unstable were close to the corresponding values for the plane-radial problem.

Thus, at certain values of Q a self-sustaining regime is generated, with successive accumulation of the liquid phase in the zone surrounding the well and its leaving the seam. The pulsatory character of this process is due to the constant inflow of heavy components into the zone around the well and their condensation, owing to which the volume of the liquid phase becomes larger. When a sufficient amount of liquid is accumulated, and it becomes sufficiently mobile, it comes to the well, the saturation profile flattens out, and so on. Let us note that in addition to the periodic regimes, at certain value of flux one observed non-damped oscillations which were not periodic in time, at least within the time considered in the calculation. The problem of stochastization of solutions of the multicomponent filtration equations requires further study (Zaslavsky 1984).

From the fact that a spatially homogeneous solution may lose its stability and from what was noted in the previous section about the continuous dependence of the solution on the boundary conditions it follows that in the inflow problems one may encounter profiles of P that are non-monotonic in the spatial coordinate. In any case, if the initial composition and pressure are such that $I(P^0, z_i^0, \ldots, z_{l-1}^0) < 0$ and the pressure at the boundary of the sink zone equals the initial one, while the pressure at the well differs from $P(R_k)$ by a sufficiently small amount, P will have non-monotonic profiles. This is confirmed by the numerical calculations made in the

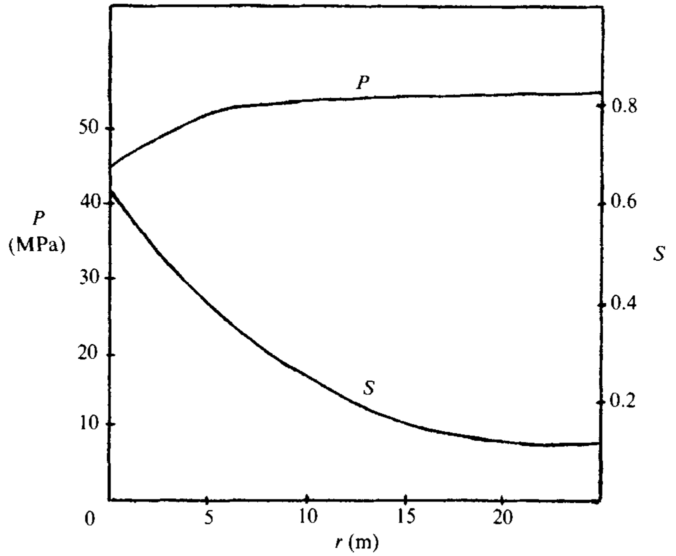

FIGURE 8. The same problem as in figure 7. Profiles of P and S.

previous section. The distributions of pressure and composition were specially calculated to study the evolution of perturbations of a spatially homogeneous solution by preliminary solution of the problem with boundary conditions for pressure of 45 and 47 MPa. As one can see in figure 1 (a), the distribution of pressure is essentially non-monotonic.

Figure 7 shows the time dependence of the mass flux debit for the gaseous and the liquid phases when the pressure at the well and at the boundary of the sink zone is respectively 45 and 55 MPa. There are no flux pulsations and the stationary regime of filtration sets in within 10 days. In the calculations where the flux at the well was fixed one observed a pulsatory regime, though the pressure at the well averaged over a period of stabilized pulsations was close to 45 MPa (see table 1). This means that it is not at all necessary that for each stable stationary solution of the problem with fixed pressure at the well there should be a corresponding stable stationary solution of the problem with fixed flux. These two problems are different. In other words, the solution essentially depends on the fixed boundary conditions. Figure 8 shows the stabilized profiles of P and S for the problem with $P(r_b, t) = 45$ MPa and $P(R_k, t) = 55$ MPa. The saturation of the liquid phase at the well coincides with the mean saturation at the well in the problem with fixed flux of 100 ton/day. However, on the whole, the profiles of S in figures 3(b) and 8 are different from each other. The stabilized value $V_g = 0.35$ is different from the period-average value for the corresponding case in table 1. The stabilized flux is $Q = 75$ ton/day and not 100 ton/day. Moreover, these values cannot be the same since such a coincidence would mean that the stationary regime also exists for a fixed flux of 100 ton/day, and this has not been observed. In our calculations with the pressures 40 and 48 MPa at the well and 55 MPa at the boundary of the drain zone, there were also no flux pulsations, but at a pressure of 25 MPa at the well the pulsations did appear.

In a series of calculations where the pressure at the well was kept equal to 46 MPa, while the pressure at the boundary of the sink zone varied, a reduction in $P(R_k)$ resulted in the appearance of pulsatory regimes. At $P(R_k, t) = 48$ MPa the stationary regime still existed, but at 47.5 MPa pulsations had already appeared. Figure 9

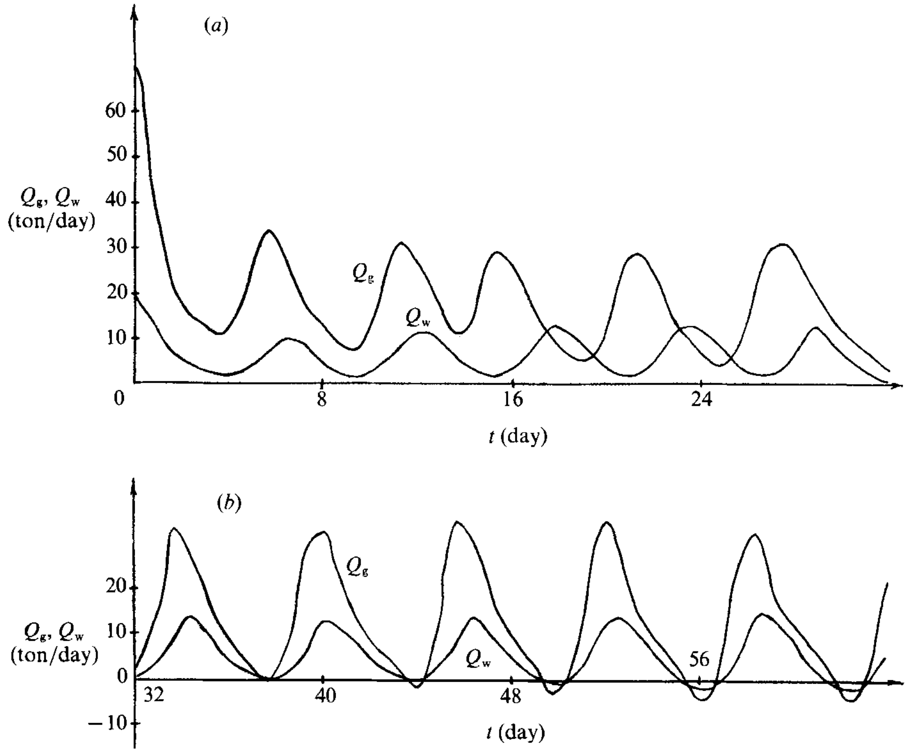

FIGURE 9. Oscillations of mass fluxes of gas and condensate in the problem with pressures of 46 and 47, 5 MPa at the boundaries.

shows the time dependence of the flux for the gaseous and the liquid phases when the pressure at the boundary of the drain zone is 47.5 MPa. The fact that P has a non-monotonic profile is indicated by the negative values of Q_g and Q_w at certain times (figure 9*b*). As was already mentioned, the non-monotonic character of the P-profile and the possibility of the flux changing its sign are both related to the fact that the problem solved here is very close to the problem of the evolution of a perturbation of a non-stable spatially homogeneous solution. Since model (2.1) makes no allowance for capillary effects at the boundary of the filtration region, at $Q < 0$ it looks as if the seam 'sucks' in the mixture in the well. The boundary effects in this model will apparently result in the sections in figure 9 where Q is negative being cut off. The well will become 'spitting': at one moment opening up and giving out products, at another shutting down. Let us note that pulsatory regimes in the calculations with sufficiently large pressure difference (e.g. $P(R_k, t) = 55$ MPa and $P(r_b, t) = 25$ MPa) did not result in a negative flux and a non-monotonic profile of P.

Let us now examine the behaviour of an important quantity, the stabilization time t_s (in those cases where the stationary solution exists). In the case of the simplest elastic filtration mode of a homogeneous liquid, described by the piezoconductivity equation, the die-away time of pressure fluctuations about the spatially homogeneous solution depends only on the initial magnitude of the fluctuation and on the piezoconductivity coefficient. The die-away time is constant at equal initial magnitudes of fluctuations for all values of the unperturbed pressure. For more complicated flowing modes or in the case of sources or sinks it seems natural enough to suppose that t_s increases as the flux becomes larger and, accordingly, the initial unperturbed state of the system moves farther away from its stationary state. The calculations made have shown that in this case t_s is a non-monotonic function of Q. Namely, one observes a significant increase of Q as one approaches the intervals where stability is lost (see table 1). Let us show that when one approaches an interval of Q-values where the stationary solution does not exist, $t_s \to \infty$ as $|Q-Q^*|^{-1}$. Here the asterisk labels the critical regime which separates the problems with a stable stationary solution from those whose stationary solution is unstable.

In the general case, the stability of a stationary regime is established by considering a certain eigenvalue problem for the operator on the right-hand side of the system of equations linearized with respect to the stationary solution. For example, for problem (2.1) this will be the system

$$\frac{k}{mN}[\nabla\cdot(\beta_i \nabla P') - z_i \nabla\cdot(\beta \nabla P')] = \lambda z_i', \quad i = 1,\ldots,l-1,$$

$$\frac{k}{m}\left(\frac{\partial N}{\partial P}\right)^{-1}\left\{\nabla\cdot(\beta\nabla P') + \sum_{j=1}^{l-1}\frac{1}{N}\frac{\partial N}{\partial z_j}[z_j \nabla\cdot(\beta\nabla P') - \nabla\cdot(\beta_i \nabla P')]\right\} = \lambda P',$$

with corresponding boundary conditions, where β_i, β and N depend on the solution of the stationary problem, and P' and z_i' are fluctuations. Suppose that at a certain value of the bifurcation parameter Q one of the eigenvalues λ crosses the imaginary axis, i.e. $\operatorname{Re}(\lambda)|_{Q=Q^*} = 0$. To be definite, let $\operatorname{Re}(\lambda) < 0$ at $Q < Q^*$ and $\operatorname{Re}(\lambda) > 0$ at $Q > Q^*$. Then, at Q close to Q^* we have

$$t_s \sim \operatorname{Re}(\lambda)^{-1} = \operatorname{Re}^{-1}\left[\lambda(Q^*) + \left.\frac{d\lambda}{dQ}\right|_{Q=Q^*}(Q-Q^*)\right] + o(Q-Q^*)$$

and

$$t_s \sim \frac{1}{|Q-Q^*|}, \quad Q < Q^*. \tag{3.1}$$

The formula for the stationary inflow of a multicomponent mixture (Khristianovich 1941) gives us

$$Q \sim H(P(R_k)) - H(P(r_b)),$$

$$|Q-Q^*| = \left|\frac{dH}{dP}(P(r_b) - P^*(r_b))\right| + o(P(r_b) - P^*(r_b)),$$

where H is the flow potential. (As is well known, for steady-state flow only one variable P is 'free': all the rest are expressed through P (Khristianovich 1941); $H = \int \beta \, dP$.) Then t_s can also be estimated as

$$t_s \sim |P(r_b) - P^*(r_b)|^{-1}. \tag{3.2}$$

Formulae (3.1) and (3.2) enable one to picture qualitatively the behaviour of $t_s(Q)$ (figure 10). As one approaches each interval of instability $(Q^*_{l,n}, Q^*_{r,n})$, hatched in the figure, t_s tends to infinity. Between $Q^*_{r,n}$ and $Q^*_{l,n+1} t_s$ is limited and passes through a minimum. Thus, in the problem considered, critical slowing down may occur before the stability is lost. Let us emphasize that the corresponding critical points in the parameter space are different from the purely thermodynamical critical point of a multicomponent liquid where all process of fluctuation resolution slow down (Ma 1976). The new critical points are essentially related to the interaction of a multicomponent system with the porous medium.

One may notice that our results concerning the non-monotonicity of the P-profile and the anomalously slow relaxation near an instability are independent of the

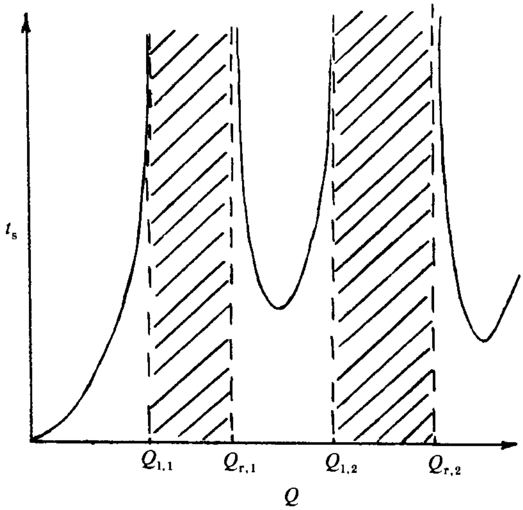

FIGURE 10. Qualitative dependence of relaxation time on an external parameter of the problem. In the hatched region the stationary solution does not exist.

specific form of system (2.1) and are due only to the very fact that unstable spatially homogeneous solutions do exist. This is why in the next section we discuss in detail the reasons why I can be negative.

4. Retrograde phenomena and negative compressibility of an individual volume

In order to understand what causes the generation of autowaves considered above one should first examine the properties of I. Figure 11 shows the calculated P-dependences of the mole density N of the mixture (curve 1), of the saturation by liquid S (curve 2) and of I (curve 3) for the composition of the multicomponent system we have presented above. Despite the fact that conditions

$$\left.\frac{\partial \rho_w}{\partial P}\right|_{x_1,\ldots,x_{l-1}} > 0, \quad \left.\frac{\partial \rho_g}{\partial P}\right|_{y_1,\ldots,y_{l-1}} > 0 \tag{4.1}$$

were satisfied, function $N(P)$ proved to be non-montonic, decreasing (except for a narrow interval 50 MPa $< P <$ 51 MPa) in the pressure range where S grows with decrease of P, i.e. in the region of retrograde condensation (the hatched region in figure 11). Thus, the condition of negative compressibility of the multicomponent mixture does not contradict the conditions of positive compressibility of individual phases, and it is in these regions that I was negative. This is not a coincidence. One may construct a hypothetical model of a multicomponent mixture with phase densities constant or only weakly depending on P (compared to S). The mass density of the mixture is

$$\tilde{N} = \rho_w S + \rho_g (1-S) = (\rho_w - \rho_g) S + \rho_g. \tag{4.2}$$

From this expression and the inequality $\rho_w > \rho_g$ it follows that in this model, at a fixed total composition, the condition $\partial\tilde{N}/\partial P < 0$ exactly corresponds to regions of retrograde condensation.

In order to understand the physical meaning of negative compressibility of a two-phase system moving in a porous medium one should turn to the known data on the thermodynamics of multicomponent systems. Figure 12(a) shows a typical

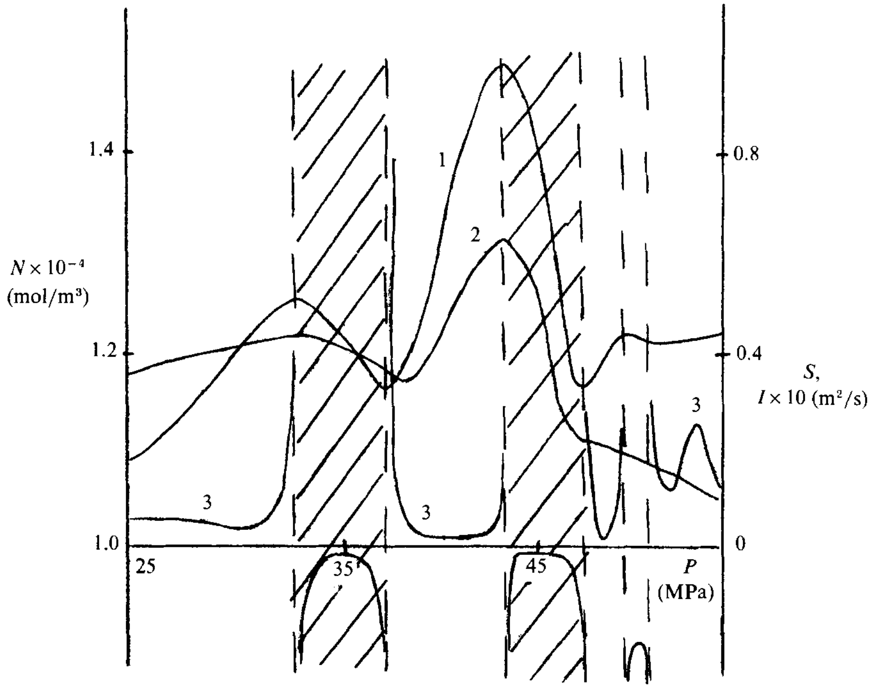

FIGURE 11. Calculated dependences of N (curve 1), S (curve 2), I (curve 3) on P for initial composition from §2 are shown.

pressure–temperature phase diagram for a mixture with constant composition. A characteristic geometric feature of such diagrams is that the section of the abscissa cut off by a vertical tangent to the boundary of the two-phase region is greater than the value of the abscissa for the critical point K and the size of the segment $0\,K'$. The properties of the curve $K'KK''$ determine the configuration of lines of equal saturation (dashed lines) so that for temperatures above the critical point $S(P)$ is non-monotonic with a decrease of P (figure 12*b*). The value of P at the point where S is maximum is called the maximum condensation pressure. The point at which the liquid appears with a decrease of P corresponds to the pressure at the beginning of condensation. The range of pressures below (above) the maximum condensation pressure corresponds to direct evaporation (to retrograde condensation).

In the context of the oil industry, the methods of finding the shape of $S(P)$-curves at fixed concentration of the mixture are called contact condensation experiments. Another popular method of studying the properties of mixtures is the so-called differential condensation. In this case, at each stage of condensation one lowers the pressure in the vessel containing the mixture and extracts the liquid that has condensed, and after that brings the rest of the mixture to the initial pressure or (in another variant of the experiment) to the initial volume. One can see that in this way one reproduces the effect of liquid condensation with the motion of an individual volume of the mixture through a porous medium. In any case, this is the generally accepted interpretation of experiments on differential condensation (Amyx, Bass & Whiting 1960).

One of the most curious effects observed in experiments on differential condensation is the so-called negative volume of heavy components, the phenomenon whereby with condensation of liquid the volume of the remaining mixture grows

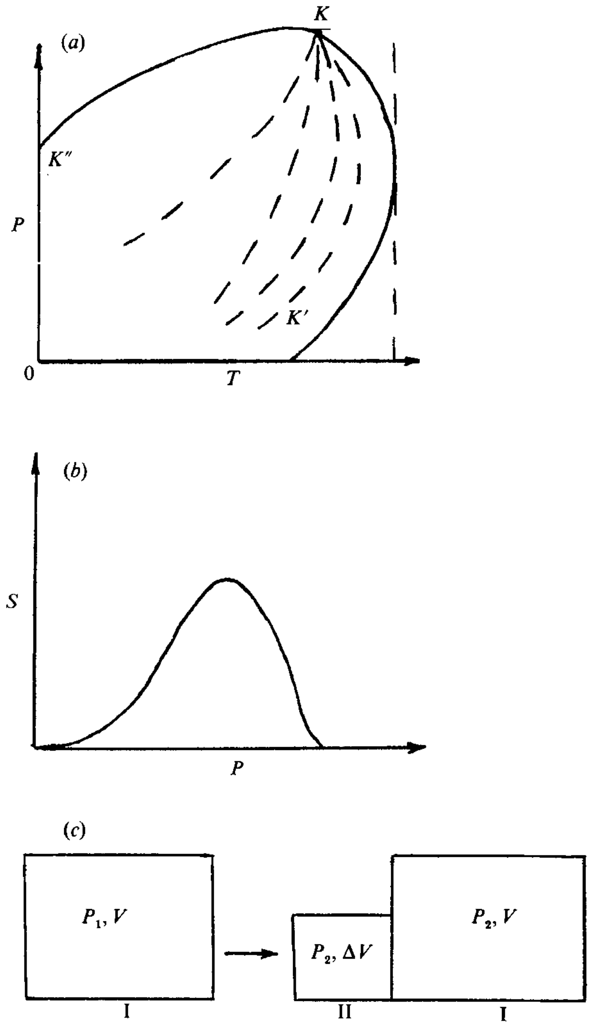

FIGURE 12. (*a*) A typical P–T phase diagram for a mixture with constant composition. (*b*) A typical dependence of S on P corresponding to the effects of retrograde condensation and direct evaporation. (*c*) The evolution of an individual volume of mixture moving in a porous medium. The effect of negative volume of heavy components leads to the negative compressibility of an individual volume ($P_2 \rightarrow P_2 > P_1$, $V + \Delta V > V$).

instead of becoming smaller (if the pressure is the same) or (if the volume is kept constant) the pressure becomes higher. Apparently, this effect was first discovered by Katz & Sliepcevic in 1945. In their experiments, which were made at fixed pressure, with successive extraction of C_{7+}, C_6, C_5, C_4, C_3, and C_2 components the volume of the mixture first increased and then (after all C_4 and heavier components have been extracted) began to diminish. Figuratively speaking, the heavy components had a sort of negative volume which, after they were extracted from the mixture, was added to the volume of the remaining system. The many experimental studies (Sage & Lacey 1950; Velikovsky & Stepanova 1962) have shown that the effect of the negative volume of heavy components is observed (i) in the regions of retrograde condensation and (ii) near the critical point of the multicomponent system. Let us note that it is the proximity to the critical point that may be the cause of a stronger dependence of S on P compared to $\rho_{w,g}$. This follows from the fact that in the near-critical state the lines of equal saturation in figure 12(a) come infinitely close to one another, which means that a small variation of P can lead to a large variation of S. In this case the model of a mixture where the phase densities change very little compared to S predicts negative compressibility in the region of retrograde condensation. Thus, the effect of negative compressibility of a mixture (figure 11) and the effect of negative volume of heavy components should take place under similar thermodynamical conditions.

Let us now show that if the multicomponent mixture is selected in such a way that in experiments on differential condensation one observes the effect of negative volume of heavy components, then the properties of such a mixture, when it moves under the same conditions through a porous medium, are described by descending density. Indeed, in the case of differential condensation we can place the liquid deposited in vessel I into vessel II. If then the volume of vessel I is brought to its initial value, the pressure in it, as was said above, will become higher than it was initially. Now let us change the volume of vessel II in such a way that the pressure in it will become equal to the new pressure in vessel I. We see that the pressure in system I+II is higher than the initial pressure in vessel I. At the same time the volume I+II is also greater than the volume of vessel I. Thus, by moving some of the molecules from one part of the system to another one can reproduce the effect of negative compressibility provided that the molecules were transferred inside the system according to their molecular weight (for instance, leaving the heavier molecules in their place).

The above two-chamber experiment was selected for a particular reason: it reflects the changes that occur in an individual volume of the mixture as it moves in the filtration flow and comes into the region where the pressure is lower than it was at the beginning of condensation (figure 12c). It is in this region that the phenomenon of the negative volume of heavy components occurs. Some of the heavy components are deposited into the initially immobile liquid phase while the lighter ones move on further. Thus, the part of the individual volume located higher upstream the flow plays the role of chamber II, while the part downstream the flow plays the role of chamber I. As was shown, for the individual volume as a whole one will observe the effect of negative compressibility which is due to the fact that the volume moves in a porous medium that acts differently upon the gaseous and the liquid phases. In the two-chamber experiment the difference in action upon different phases is simply due to the gravitational separation of substances with different densities.

The above considerations show that when describing the hydrodynamics of a two-phase mixture in a porous medium in the region of retrograde condensation one should take into account the possible descending of the mixture density. This becomes especially evident when one describes the flow not with Eulerian coordinates, which are secondary, but with Lagrange coordinates, which are primary in continuum mechanics and are designed for describing the evolution of an individual volume. It is also important that when we use a continuous description like (2.1), we are dealing with quantities averaged over a large number of pore channels. In some of the channels belonging to the averaging volume differential condensation may occur, while the others will be filled with lighter components carried away along the flow. Thus, the appearance of a descending density branch in the thermodynamics of an individual volume of a two-phase mixture moving in a porous medium seems to be not only natural but also inevitable. The scheme presented of the experiment with a two-chamber model gives one, in the first approximation, a method of determining the descending density branch under laboratory conditions.

5. From a non-equilibrium model of multicomponent filtration to a model with local equilibrium

Let us now see how the results obtained above change as we turn to more complete models of filtration. As is easily seen, the introduction of terms into system (2.1) that are responsible for capillary and diffusion effects, and are small compared to the terms describing convective transfer, will not affect the possibility of I changing its sign due to its denominator running through zero, if such a possibility existed initially in model (2.1). The account of the non-equilibrium character of interphase transfer is another matter. Let us examine this problem more closely and show that the account of non-equilibrium effects regularizes problem (2.1) in a situation where the quantity $\partial N/\partial P|_{z_1,\dots,z_{l-1}}$ may change its sign, and in the framework of model (2.1) we have (relaxation) oscillations discontinuous in time.

One may start with the system of equations of the form (Nikolaevsky *et al.* 1968; Rozenberg *et al.* 1969)

$$m\frac{\partial N z_i}{\partial t} = \nabla\cdot(k\beta_i\nabla P), \quad i = 1,\dots,l, \tag{5,1}$$

$$m\frac{\partial N_g y_i}{\partial t} = \nabla\cdot(k\beta_i^g\nabla P)+\tau^{-1}\varphi_i, \quad i = 1,\dots,l. \tag{5.2}$$

This system is a generalization of (2.1) to the case of non-equilibrium multicomponent filtration. Here $N_g = \rho_g(1-S)/M_g$; β_i^g is the part of β_i corresponding to the motion of the gas; and τ is the characteristic relaxation time for interphase mass exchange. In the general case we have a set of quantities τ_i for each component. Quantity φ_i measures the deviation from phase equilibrium in the ith component and, according to the relations of non-equilibrium thermodynamics, is proportional to the difference of chemical potentials of the ith components in the liquid and gaseous phases,

$$\sum_{i=1}^{l} y_i = \sum_{i=1}^{l} z_i = 1.$$

In the zeroth approximation with respect to τ, (5.1) and (5.2) give system (2.1) with the closing constraints

$$\varphi_i = 0, \quad i = 1,\dots,l. \tag{5.3}$$

Relations (5.3) are equivalent to (2.3) (Read *et al.* 1977). For system (5.1) and (5.2), the unknown quantities are $\boldsymbol{u} = (z_1,\dots,z_{l-1},P)$ and $\boldsymbol{v} = (y_1,\dots,y_{l-1},S)$. In the local-equilibrium model (5.1), (5.3), $\boldsymbol{v}$ can be expressed through $\boldsymbol{u}$ using relations (5.3), and thus at $\tau = 0$ the unknown quantities are $\boldsymbol{u}$.

By considering the problem of the linear stage of the evolution of perturbations of a spatially homogeneous solution of system (5.1), (5.2) in the region shaped like a rectangular parallelepiped with dimensions L_j, it is easy to show that condition (4.1) is sufficient for the elements of the linear response matrix not to have poles. This holds for any $\tau > 0$ but at $\tau = 0$, as was shown above, despite the fact that condition (4.1) is satisfied, the denominator of I can become zero. Since the transition from (5.1) and (5.2) to (5.1) and (5.3) occurs at $\tau \to 0$, it is natural to examine this transition using the method of perturbations.

By linearizing (5.2) and considering the Fourier components of fluctuations, $\boldsymbol{u}'_q$ and $\boldsymbol{v}'_q$, instead of (5.2) we get

$$\tau\left(\boldsymbol{A}\frac{\mathrm{d}\boldsymbol{u}'_q}{\mathrm{d}t}+\boldsymbol{B}\frac{\mathrm{d}\boldsymbol{v}'_q}{\mathrm{d}t}\right)=-\tau q^2\boldsymbol{C}\boldsymbol{u}'_q+\boldsymbol{E}\boldsymbol{u}'_q+\boldsymbol{F}\boldsymbol{v}'_q. \tag{5.4}$$

Here q^2 is the wave vector squared; $\boldsymbol{A}$, $\boldsymbol{B}$, $\boldsymbol{C}$, $\boldsymbol{E}$, and $\boldsymbol{F}$ are $l\times l$ matrices depending on the spatially homogeneous solution. The structure of these matrices is determined by (5.2). For instance, $\boldsymbol{E}$ and $\boldsymbol{F}$ are matrices of the first derivatives of φ_i with respect to components of vectors $\boldsymbol{u}$ and $\boldsymbol{v}$. By using (5.4) one can show that, up to the second-order terms in τ, $\boldsymbol{v}'_q$ is expressed through $\boldsymbol{u}'_q$ in the following way:

$$\boldsymbol{v}'_q=-\boldsymbol{F}^{-1}\boldsymbol{E}\boldsymbol{u}'_q+q^2\tau\boldsymbol{F}^{-1}\boldsymbol{C}\boldsymbol{u}'_q+\tau(\boldsymbol{F}^{-1}\boldsymbol{A}-\boldsymbol{F}^{-1}\boldsymbol{B}\boldsymbol{F}^{-1}\boldsymbol{E})\frac{\mathrm{d}\boldsymbol{u}'_q}{\mathrm{d}t}. \tag{5.5}$$

Let us note that if one makes the transformation to originals in (5.5), one will get a relation between $\boldsymbol{u}$ and $\boldsymbol{v}$ involving both time and space derivatives. The existence of matrix $\boldsymbol{F}^{-1}$ follows from the implicit function theorem for $\boldsymbol{\phi}=0$ and from the fact that in the model (5.1), (5.3) $\boldsymbol{v}$ can always be expressed through $\boldsymbol{u}$ using (5.3).

After linearization and transition to Fourier components of fluctuations, system (5.1) acquires the form

$$\boldsymbol{D}\frac{\mathrm{d}\boldsymbol{u}'_q}{\mathrm{d}t}+\boldsymbol{M}\frac{\mathrm{d}\boldsymbol{v}'_q}{\mathrm{d}t}=-q^2\boldsymbol{G}\boldsymbol{u}'_q, \tag{5.6}$$

where $\boldsymbol{D}$, $\boldsymbol{M}$, and $\boldsymbol{G}$ are $l\times l$ matrices. By substituting (5.5) into (5.6) we obtain

$$\tau\boldsymbol{M}\boldsymbol{F}^{-1}(\boldsymbol{A}-\boldsymbol{B}\boldsymbol{F}^{-1}\boldsymbol{E})\frac{\mathrm{d}^2\boldsymbol{u}'_q}{\mathrm{d}t^2}+[(\boldsymbol{D}-\boldsymbol{M}\boldsymbol{F}^{-1}\boldsymbol{E})+\tau q^2\boldsymbol{M}\boldsymbol{F}^{-1}\boldsymbol{C}]\frac{\mathrm{d}\boldsymbol{u}'_q}{\mathrm{d}t}+q^2\boldsymbol{G}\boldsymbol{u}'_q=0. \tag{5.7}$$

At $\tau=0$, from (5.7) one should obtain the linearized system (5.1)–(5.3) expressed in terms of Fourier components of fluctuations, or, equivalently, system (2.1)–(2.4). Transforming (5.7) in such a way that the matrix that stands in front of $\mathrm{d}\boldsymbol{u}'_q/\mathrm{d}t$ and does not depend on q^2 becomes diagonal (this is achieved by the same transformations as those used in §2 for transforming the initial linearized system (2.1) into system (2.8)), we obtain

$$\tau\boldsymbol{R}^{\mathrm{I}}\frac{\mathrm{d}^2\boldsymbol{u}'_q}{\mathrm{d}t^2}+(\boldsymbol{R}^{\mathrm{II}}+\boldsymbol{R}^{\mathrm{III}}q^2\tau)\frac{\mathrm{d}\boldsymbol{u}'_q}{\mathrm{d}t}+q^2\boldsymbol{R}^{\mathrm{IV}}\boldsymbol{u}'_q=0, \tag{5.8}$$

where $\boldsymbol{R}^n=\{r^n_{ij}\}$ are square matrices of order l. Thus, instead of $2l$ equations (5.1), (5.2) we obtain l equations of the second order in t, with the initial conditions for $\mathrm{d}\boldsymbol{u}'_q/\mathrm{d}t$ found from the initial conditions for system (5.1), (5.2), and (5.5). Comparing (5.8) at $\tau=0$ with (2.8), we find

$$\boldsymbol{R}^{\mathrm{II}}=\begin{pmatrix}1 & & 0\\ & \ddots & \\ 0 & & \dfrac{\partial N}{\partial P}\end{pmatrix},\quad \boldsymbol{R}^{\mathrm{IV}}=\begin{pmatrix}0\ldots0 & r^{\mathrm{IV}}_{1l}\\ \vdots\quad\vdots & \vdots\\ 0\ldots0 & r^{\mathrm{IV}}_{ll}\end{pmatrix},$$

$$r^{\mathrm{IV}}_{il}=\frac{1}{mN}(\beta_i-z_i\beta),\quad i=1,\ldots,l-1,$$

$$r^{\mathrm{IV}}_{ll}=\frac{k}{m}\left[\beta-\frac{1}{N}\sum_{j=1}^{l-1}\frac{\partial N}{\partial z_j}(\beta_j-z_j\beta)\right].$$

The form of matrices $\mathbf{R}^{\mathrm{II}}$ and $\mathbf{R}^{\mathrm{III}}$ is unessential for what follows.

Now we notice that, up to the τ^2-terms, for obtaining the equation for $P'_q = u'_{q,l}$ one should substitute the zeroth approximation of $u'_{q,i}$ ($i = 1, \ldots, l-1$) into the last line in (5.8). We obtain

$$\tau d_1 \frac{\mathrm{d}^2 P'_q}{\mathrm{d}t^2} + \left(\frac{\partial N}{\partial P} + q^2 \tau d_2\right) \frac{\mathrm{d}P'_q}{\mathrm{d}t} + q^2 d_3 P'_q = 0, \tag{5.9}$$

where
$$d_1 = r^{\mathrm{I}}_{ll}, \quad d_2 = r^{\mathrm{III}}_{ll} - \sum_{i=1}^{l-1} r^{\mathrm{I}}_{li} r^{\mathrm{IV}}_{il}, \quad d_3 = r^{\mathrm{IV}}_{ll}.$$

The expression for d_2 is obtained by taking account of the fact that both $\mathbf{R}^{\mathrm{III}}$ and $\mathbf{C}$ have non-zero elements only in their lth column.

Thus, the proximity of $\partial N/\partial P$ to zero makes it necessary to take into account the second-order time derivatives in the equation for P, i.e. to take into account the non-equilibrium effects. By comparing (5.9) and (2.8), one can see that the condition $I^{-1} = 0$ in the local-equilibrium model at $d_1 d_3 > 0$ and $\partial N/\partial P + q^2 \tau d_2 = 0$ corresponds, in the non-equilibrium model, to the moment at which the time-periodic solutions of small amplitude appear. If, in addition, we have $d_2 > 0$, then all the conditions necessary for continuation of periodic solutions into the region of instability in the problem considered are satisfied. Indeed, from (5.9) it follows that in the given problem the eigenvalues are found, up to the τ^2 terms, from the equation

$$\tau d_1 \lambda^2 + \left(\frac{\partial N}{\partial P} + q^2 \tau d_2\right) \lambda + q^2 d_3 = 0. \tag{5.10}$$

If a pair of eigenvalues corresponding to the minimum value of the wave vector squared,

$$q_*^2 = \frac{4\pi^2}{\sum_{j=1}^{d} L_j^2}$$

is purely imaginary (according to (5.10), this will happen at $-\partial N/\partial P = q_*^2 \tau d_2$), then all the modes with smaller wavelength ($q^2 > q_*^2$) will have eigenvalues lying in the left half-plane. According to Hopf's theorem for distributed systems (Marsden & McCracken 1976), the periodic orbit corresponding to q_*^2 can be continued into the region $\partial N/\partial P < -q_*^2 \tau d_2$.

The period of the auto-oscillations generated from (5.9), equals

$$T_{\mathrm{p}} = 2\pi \left(\frac{\tau d_1}{q_*^2 d_3}\right)^{\frac{1}{2}}, \tag{5.11}$$

i.e. is proportional to the spatial scale of fluctuations and to the square root of τ. By analysing the structure of coefficients d_1 and d_3 in (5.11) more closely one can show that the period of auto-oscillations is of the order of the geometric mean of the characteristic phase equilibrium time τ and the characteristic time of transfer of a mixture particle in the filtration flow along the solution region τ_{f}:

$$T_{\mathrm{p}} \sim (\tau \tau_{\mathrm{f}})^{\frac{1}{2}}.$$

Thus, if the auto-oscillations are generated in a region of size around 1 m (e.g. in the zone surrounding a well) and have a period of about 1 hour, the auto-oscillations at the scale of the deposit (kilometres) will have a period of around a month.

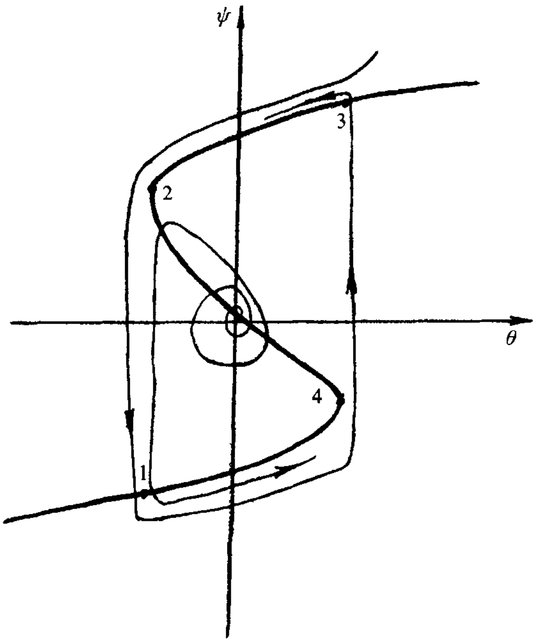

FIGURE 13. Relaxation oscillations in the one-mode approximation: the phase plane is constructed from (5.13).

In the one-mode approximation, the nonlinear equation for P'_q corresponding to the linearization of (5.9) will have the form

$$\left.\begin{aligned} &\tau d_1 \frac{\mathrm{d}^2 P'_q}{\mathrm{d}t^2} + \frac{\mathrm{d}W(P'_q)}{\mathrm{d}t} + q^2 d_3 P'_q = 0, \\ &W(P'_q) = q^2 \tau d_2 P'_q + \frac{\partial N}{\partial P} P'_q + \frac{1}{2}\frac{\partial^2 N}{\partial P^2}(P'_q)^2 + \frac{1}{6}\frac{\partial^3 N}{\partial P^3}(P'_q)^3. \end{aligned}\right\} \tag{5.12}$$

This equation is obtained by keeping the terms nonlinear in P' in the function $N(P)$ in the vicinity of the spatially homogeneous solution with $\partial N/\partial P \approx 0$. It is close to the Van der Pol equation and at $\partial^2 N/\partial P^2 = 0$ coincides with it exactly (Andronov, Vitt & Khaikin 1982). Like the Van der Pol equation, (5.12) can be examined from the viewpoint of the theory of relaxation oscillations. Let us present (5.12) in the form of equivalent systems:

$$\left.\begin{aligned} &d_1 \frac{\mathrm{d}\psi}{\mathrm{d}t_1} = \theta - W(\psi), \qquad && \tau d_1 \frac{\mathrm{d}\psi}{\mathrm{d}t} = \theta - W(\psi), \\ &\frac{\mathrm{d}\theta}{\mathrm{d}t_1} = -\tau d_3 q^2 \psi, && \frac{\mathrm{d}\theta}{\mathrm{d}t} = -\psi q^2 d_3, \end{aligned}\right\} \tag{5.13}$$

where $\psi = P'_q$; $t_1 = t/\tau$ is the short timescale. Figure 13 shows the phase plane of (5.13). The limit $\tau = 0$ in the right-hand side of (5.13) describes the fast motion along sections 1–2 and 3–4 of the plane trajectory. The slow motion along 2–3 and 1–4 is described by equations of the second system in (5.13) at $\tau = 0$. Taking the limit $\tau = 0$ in the 'slow' system in (5.13) leads to instantaneous relaxation of the solution in the vicinity of points 1, 2, 3, and 4, corresponding to zero compressibility, and the motion is described as being piecewise discontinuous with sections where parameters vary monotonically, alternating with discontinuities. At small non-zero τ the auto-oscillations will have the form of alternating fast and slow motions. It is noteworthy that here the fast motions correspond to crossing of regions of retrograde condensation in the space of thermodynamical parameters, while the slow motions are associated with regions of direct evaporation. Let us note that this picture corresponds to keeping only one mode in the nonlinear description. The calculations made in §§2 and 3 show that there may be more complicated autowave regimes corresponding to the interaction between several modes.

6. Discussion of experimental results and conclusions

We thus see that the possibility of autowave generation is related to the loss of stability of stationary solutions of equations of two-phase multicomponent filtration. According to the above considerations, the loss of stability in a distributed system should occur in the region of retrograde condensation. The self-sustaining oscillations should be generated owing to the cyclic alternation of the following processes: (i) accumulation of the liquid phase in the region of space corresponding to retrograde condensation, (ii) transport of the liquid in the filtrational flow into the region corresponding to evaporation, and (iii) the diminishing of the volume occupied by the liquid phase in this latter region. It is predicted that there may be non-monotonic profiles of pressure and the anomalous increase of the time within which the stationary regime sets in as one of the parameters approaches the region of instability. This process may have the character of autowaves in an open system, i.e. under continuous inflow of energy from outside.

The results presented have been mainly obtained in 1985, were reported at the 6th All-Union Conference on Mechanics in 1986 and were published as a short report in 1987. The next step was to obtain experimental confirmation of the theory. We do not mean the observation of fluid auto-oscillations with exploitation of deposits – there have been plenty of such observations already. The principal idea was to do experiments under laboratory conditions in the range of parameters predicted by the theory. Such experiments were performed in 1988 by B. V. Makeev. A complete account of the results obtained is presented in our paper (Makeev & Mitlin 1990). Here I shall mention only the most important confirmations of the theory obtained in these experiments.

The experiments were done with a linear model of a seam with a porous medium poured on. The pressure at the inlet was kept constant and equal to 13.4 MPa (the system was open). The simulation was done at 296.5 K, with a multicomponent mixture for which the filtration occurs both in the regime of retrograde condensation and in the direct evaporation regime, depending on the pressure at the given point of the linear model of a seam. The mixture is characterized by the pressure at the beginning of condensation 12.7 MPa and by the maximum condensation pressure 12 MPa. The system was brought into the working regime by lowering the pressure in the model from 15 MPa.

Two experiments were performed. In the first the pressure at the inlet of the linear model was 9.4 MPa. Figure 14 shows the time variation of pressure at different points of the model. The ith curve corresponds to measurements made at the point with coordinates $r_i = (i/6)L$. One can see that there are damped oscillations of pressure, their amplitude being the greater the closer the measurement point is to the exit of the

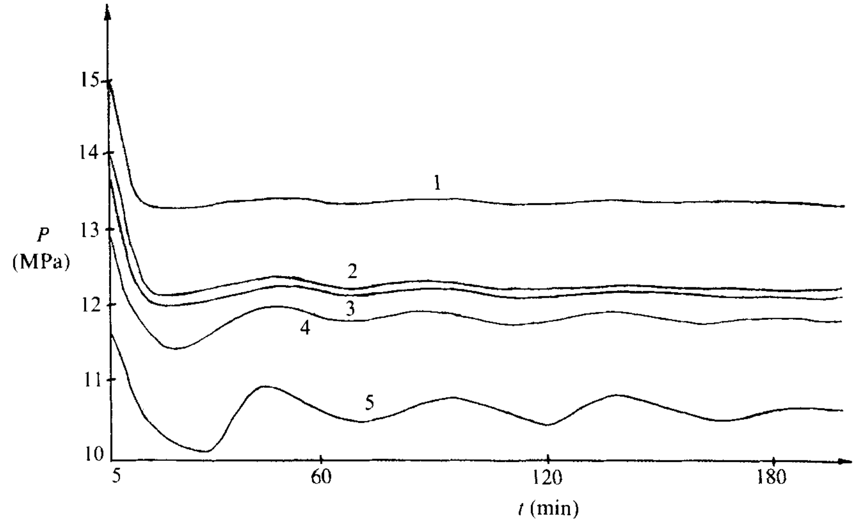

FIGURE 14. Dynamics of P at different points of the model of a seam (experiment 1). For curve labelling, see text.

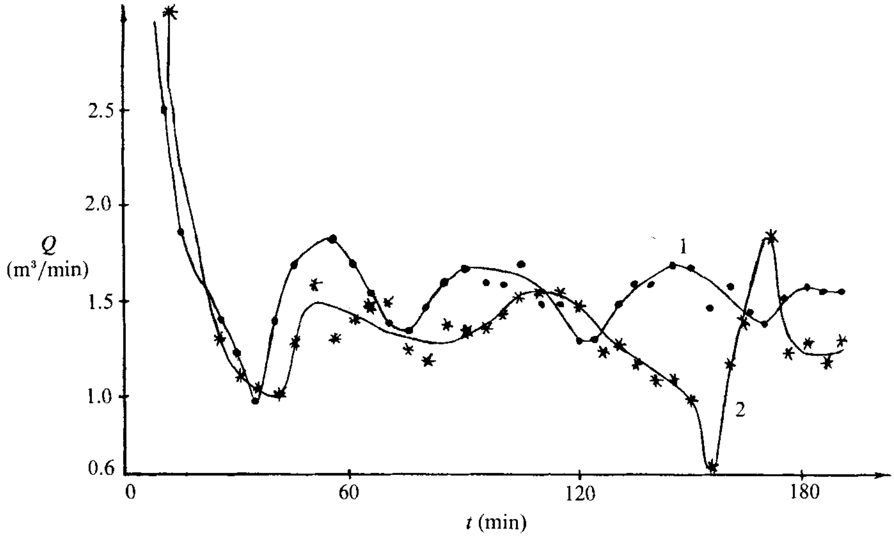

FIGURE 15. Dynamics of the flow velocity at the exit of the model (curve 1 corresponds to the first experiment, 2 to the second one).

model. At the point r_5 the amplitude of oscillations reached 0.9 MPa. The profiles of P change little along the seam when the pressure is around the pressure at the beginning of condensation or around the maximum condensation pressure.

A chromatographic analysis of the mixture coming out of the seam has shown that there are oscillations of composition in the flow.

Figure 15 shows the time variation of the flow velocity at the exit of the model (curve I). The characteristics of the rate at the exit, Q, were measured here in units of m^3/min at $T = 296.5$ K and $P = 0.1$ MPa. The velocity oscillations have a period of 40 min. The maximum values of velocity correspond to minima in curve 5 (figure 14), and vice versa. The oscillations die away in about 3 to 3.5 hours.

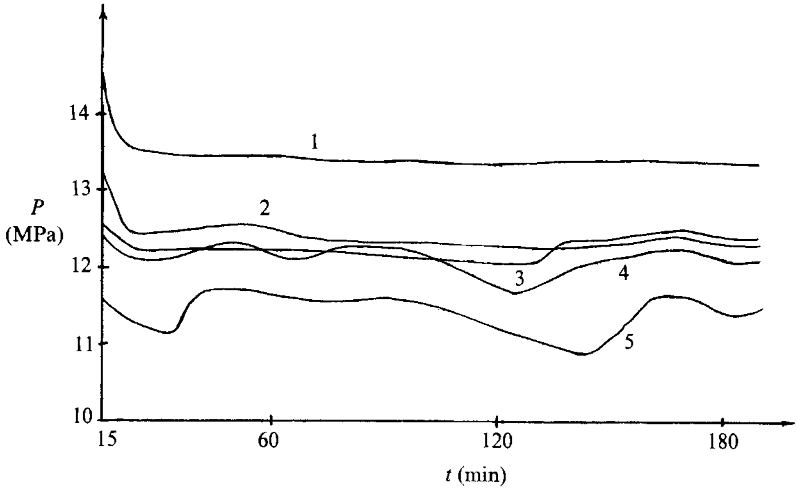

FIGURE 16. Dynamics of P at different points of the model of a seam (experiment 2). Labelling corresponds to figure 14.

In the second experiment the pressure at the exit of the model was fixed at 10.6 MPa. All other parameters were the same. Figure 16 shows the time variation of pressure at different points of the model. The labelling of the curves corresponds to that in figure 14. Despite the fact that the difference in pressure between the ends of the model is one and a half times smaller than in the first experiment, the process now is much more complicated. One could very clearly observe that the pressure at the points located closer to the exit was constantly higher than it was at the points located farther away from the exit (the overlapping of curves 2, 3 and 3, 4). The oscillations at the point r_5 had a clearly distinguished period of about 2 hours. The amplitude of oscillations reached 0.8 MPa. At times where the oscillations in the first experiment died away, no damping of autowaves was now observed. According to our theory, this is an indication of the relaxation processes slowing down as the region of non-stable stationary solutions is approached.

Curve 2 in figure 15 shows the time dependence of the velocity at the exit. The velocity reaches its minimum at $t = 40$ min. After that, against a background of small-scale oscillations, a slow increase of velocity occurs, which is then replaced first by a slow and then by a more rapid decrease. The minimum of velocity is reached at $t = 155$ min, and this minimum is much deeper than the first one. After that the velocity rises, which corresponds to cyclic resumption of auto-oscillations. Such behaviour of the velocity is associated with a slow accumulation of the liquid phase replaced by abrupt 'shutting down' of the filtration flow, and then by the emergence of the liquid phase that has acquired sufficient mobility.

Thus, the autowaves in the case of filtration with phase transitions have been experimentally observed. The results of these experiments confirm the following predictions of the theory.

The autowaves can be observed in an open system if the region of the flow consists of areas corresponding to retrograde condensation and to evaporation processes.

In those regions of the flow that correspond to retrograde condensation, the pressure may have non-monotonic profiles. According to the considerations of §4, this suggests an actual observation of the effect of negative compressibility of an individual volume of the moving mixture.

The non-monotonic profiles were observed only when the pressure difference between the ends of the model was smaller (i.e. in the second experiment). This agrees remarkably well with the results of calculations presented in §3, where the pressure at one of the ends corresponded to an unstable spatially homogeneous solution, the pressure difference between the ends was varied, and non-monotonic profiles of P were observed only for sufficiently small pressure difference.

The relaxation time in the system grows as the instability is approached: in this case the parameter that determines the proximity of the system to the instability region is the deviation of pressure at the exit from the maximum condensation pressure. This result is very significant in confirming the theory, since in the second experiment it was natural to expect a more rapid damping of oscillations. This would have been the case if we were dealing with a one-phase liquid moving in the porous medium and filtration occurred without phase transitions. As one can see, the phase transitions in the filtration process can significantly change the situation.

Thus, one more example of self-organization in dynamical systems has been discovered and described. Let us note that the succession of events that have led to the results presented above was the following. First, in calculations with the data from a real deposits† we have numerically observed the autowave regimes. Then we have constructed a theory of these phenomena and, finally, this theory was confirmed experimentally. In our opinion, this course of events may serve as an additional confirmation of the correctness of our theory.

However, it is necessary to undertake a programme of investigation of autowave filtration flows. The programme must include investigations of the thermodynamical properties of mixtures in retrograde conditions (in particular, experiment with descending density branch are considered in §4), experimental investigations of the hydrodynamics of multicomponent fluids in porous media for retrograde conditions and, finally, improvement of numerical methods of solving multicomponent filtration equations. Our numerical method used above permits regions of instability to be found and the dynamics of autowaves to be described. However, it was not specially aimed at calculation of time-discontinuities (relaxation) processes. In a simple case this can be illustrated by 'slow' Van der Pol equation

$$(1-\psi^2)\frac{d\psi}{dt} = \psi. \tag{6.1}$$

It is obvious that any direct numerical method leads to the accuracy loss near discontinuous points $\psi = \pm 1$. Two approaches to correction are possible. Firstly, the term $\sim d^2\psi/dt^2$ should be added to (6.1) and then one can solve the full Van der Pol equation. For the problem of multicomponent filtration it means solving general equations (5.1), (5.2). Secondly, (2.1) can be solved with control of the value $\partial N/\partial P$ at any sites of the different grid ($|\partial N/\partial P| > \epsilon$). We hope to consider these questions in detail in a future publication.

The author is very grateful to V. N. Nikolaevsky and B. V. Makeev for useful discussions of this work.

---

† In 1985 I carried out calculations of problems of stationary inflow to a well for deposit Karachaganak. However, it was found that for some initial conditions a stationary solution could not exist. Later I learnt that the same effects impeding the use of standard methods of well testing had in fact been observed for Karachaganak.

REFERENCES

Amyx, J. W., Bass, D. M. & Whiting, J. R. Z. 1960 *Petroleum Reservoir Engineering: Physical Properties*. McGraw-Hill.

Andronov, A. A., Vitt, A. A. & Khaikin, S. E. 1982 *Theory of Oscillations*. Moscow: Nauka (in Russian).

Aziz, K. & Settari, A. 1979 *Petroleum Reservoir Simulation*. London: Applied Science Publishers.

Barenblatt, G. I., Entov, V. M. & Ryzhik, V. M. 1984 *Motion of Liquids and Gases in Natural Seams*. Moscow: Nedra (in Russian).

Collins, R. E. 1961 *Flow of Fluids through Porous Materials*. Reinhold: Chapman & Hall.

Haken, G. 1983 *Synergetics. An Introduction*. Springer.

Katz, D. L. & Sliepcevic, C. M. 1945 *The Oil Weekly* **116** (13), 30.

Khristianovich, S. A. 1941 On the motion of aerated liquid in porous rocks. *Prikl. Matem. i Mekh.* **5**, 277–282.

Landau, L. D. & Lifshitz, E. M. 1986 *Hydrodynamics*. Moscow: Nauka (in Russian).

Ma, S. 1976 *Modern Theory of Critical Phenomena*. Reading MA: W. A. Benjamin Inc., Advanced Book Program.

Makeev, B. V. & Mitlin, V. S. 1990 Autooscillations in distributed systems: filtration with phase transitions. *Dokl. Akad. Nauk SSSR* **310**, 1315–1319.

Marsden, J. E. & McCracken, M. 1976 *The Hopf Bifurcation and its Applications*. Springer.

Mitlin, V. S. 1986*a* Autooscillational regimes of multicomponent filtration of mixtures. In *Theses of Talks presented at the 6th All-Union Conference on Theoretical and Applied Mechanics, Tashkent*, p. 458 (in Russian).

Mitlin, V. S. 1986*b* A method of numerical solution of one- and two-dimensional problems of multicomponent filtration without iterations. In *Numerical Methods in Continuum Mechanics*, vol. 17, No. 4, pp. 110–129. Novosibirsk: ITPM SO AN SSSR (in Russian).

Mitlin, V. S. 1987*a* New methods of calculation of the enriched gas action upon a gas-condensate seam. Summary of Doctoral Thesis, Moscow, p. 24 (in Russian).

Mitlin, V. S. 1987*b* Autooscillational flowing regimes of two-phase multicomponent mixtures through porous media. *Dokl. Akad. Nauk SSSR* **296**, 1323–1327.

Nicolis, G. & Prigogine, I. 1977 *Self-Organization in Nonequilibrium Systems*. Wiley.

Nikolaevsky, V. N., Bondarev, E. A., Mirkin, M. I., Stepanova, G. S. & Tersi, V. P. 1968 *Motion of Hydrocarbon Mixtures in Porous Media*. Moscow: Nedra (in Russian).

Read, R. S., Prausnitz, J. M. & Sherwood, T. K. 1977 *The Properties of Gases and Liquids*. McGraw-Hill.

Rosenberg, M. D., Kundin, S. A., Kurbanov, A. K., Suvorov, N. I. & Shovkrinsky, G. Yu. 1969 *Filtration of Gased Liquids and Other Multicomponent Mixtures in Oil Seams*. Moscow: Nedra (in Russian).

Sage, B. H. & Lacey, W. N. 1950 *Thermodynamic Properties of the Lighter Paraffin Hydrocarbons and Nitrogen*. American Petroleum Institute.

Velikovsky, A. S. & Stepanova, G. S. 1962 Negative volume of the less volatile component in methane mixtures with different hydrocarbons. In *The Study of Gas-Condensate Deposits, Proc. VNIIGAZ, Moscow*, No. 17/25, pp. 232–253 (in Russian).

Yuen, H. C. & Lake, B. M. 1978 In *Solitons in Action* (ed. K. Lonngren & A. Scott), pp. 89–126. Academic.

Zaslavsky, G. M. 1984 *Stochasticity of Dynamical Systems*. Moscow: Nauka (in Russian).